Pharmacogn. Mag.
A multifaceted peer reviewed journal in the field of Pharmacognosy and Natural Products
www.phcog.com | www.phcog.net

ORIGINAL ARTICLE

Systems Bioinformatic Approach to Determine the Pharmacological Mechanisms of *Radix Astragali* and *Radix Angelicae sinensis* in Idiopathic Pulmonary Fibrosis

Yufeng Zhang[1,2,3], Lina Gu[1,3], Juan PuYang[3], Mengying Liu[4], Qingqing Xia[2], Weilong Jiang[2], Mengshu Cao[1,3,4]

[1]Department of Pulmonary and Critical Care Medicine, Nanjing Drum Tower Hospital Clinical College of Traditional Chinese and Western Medicine, Nanjing University of Chinese Medicine, Nanjing, [2]Department of Respiratory Medicine, Jiangyin Hospital of Traditional Chinese Medicine, Jiangyin Hospital Affiliated to Nanjing University of Chinese Medicine, Jiangyin, [3]Department of Pulmonary and Critical Care Medicine, Nanjing Drum Tower Hospital, The Affiliated Hospital of Nanjing University Medical School, [4]Department of Pulmonary and Critical Care Medicine, Nanjing Drum Tower Hospital Clinical College of Nanjing Medical University, Nanjing, China

Submitted: 07-Jan-2021 Revised: 10-Apr-2021 Accepted: 06-May-2021 Published: 24-Jan-2022

ABSTRACT

Background: Earlier meta-analysis has publicized that *Radix Astragali (*RA) and *Radix Angelicae sinensis* (RAS) are valuable to pulmonary function and exercise capacity in patients with idiopathic pulmonary fibrosis (IPF). **Objectives:** The objective of the study was to regulate the pharmacological mechanism of RA and RAS in IPF treatment. **Materials and Methods:** Microarray datasets for IPF were examined in the Gene Expression Omnibus database and differentially expressed genes (DEGs) were recognized. Active compounds and target genes of RA and RAS were recognized using the Traditional Chinese Medicine Systems Pharmacology platform. The DEGs were combined with the active target genes to construct a medicine-compound-gene network and a protein–protein interaction network using Cytoscape software. Gene ontology function enrichment and Kyoto Encyclopedia of Genes and Genomes pathway enrichment were studied using RGUI. A gene-pathway network was established using Cytoscape and molecular docking was done using AutoDock Tool and AutoDock Vina software. **Results:** We recognized 1566 DEGs and 40 candidate target genes of RA and RAS acting on IPF. The six key active compounds prophesied were quercetin, kaempferol, stigmasterol, 7-O-methylisomucronulatol, formononetin, and beta-sitosterol. Following network construction and enrichment, the two main pathways were acknowledged, namely the tumor necrosis factor signaling pathway and advanced glycation end (AGE) products receptor for AGE signaling pathway. Preliminary molecular docking to confirm interactions between key compounds and their protein targets in the pathways was carried out. **Conclusion:** The pharmacological mechanisms of RA and RAS in IPF treatment have been further elucidated, which could show valuable in future studies on their mechanisms of action for the treatment of IPF.

Key words: Idiopathic pulmonary fibrosis, Kyoto Encyclopedia of Genes and Genomes pathway, molecular docking, network pharmacology, *Radix Angelicae sinensis, Radix Astragali*

SUMMARY

- *Radix Astragali* (RA) and *Radix Angelicae sinensis* (RAS) are promising to pulmonary function and exercise capacity of patients with idiopathic pulmonary fibrosis (IPF). First, we scrutinized microarray datasets for differentially expressed genes (DEGs) in IPF tissues compared with normal tissues. Next, we documented the active compounds and target genes of RA and RAS. Then, we combined the DEGs with the active target genes to build a medicine-compound-gene network and protein–protein interaction network. Next, we had done gene ontology function enrichment and Kyoto Encyclopedia of Genes and Genomes pathway enrichment. Finally, a gene-pathway network for IPF was effectively recognized and the interactions between key compounds and their protein targets were confirmed by molecular docking. The pharmacological mechanisms of RA and RAS in IPF treatment have been further elucidated, which could validate valuable in upcoming studies on their mechanism of action for the treatment of IPF.

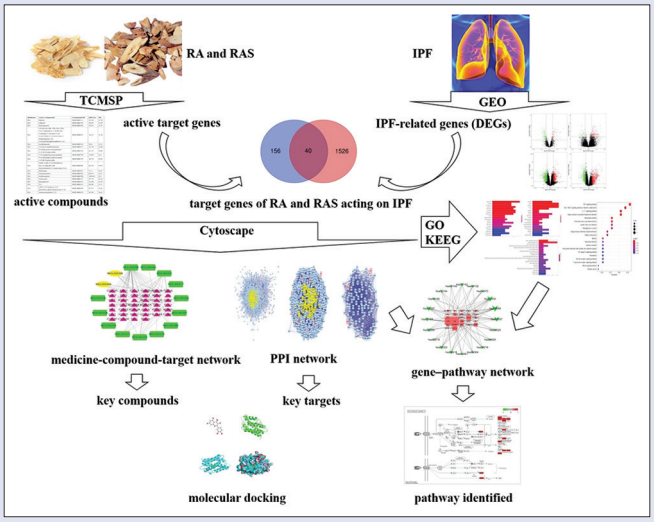

Abbreviations used: RA: *Radix Astragali*; RAS: *Radix Angelicae sinensis*; IPF: idiopathic pulmonary fibrosis; DEGs: differentially expressed genes; AGE: advanced glycation end; TCM: Traditional Chinese medicine; PPI: protein-protein interaction; GO: Gene Ontology; KEGG: Kyoto Encyclopedia of Genes and Genomes; NCBI: National Center for Biotechnology Information; GEO: Gene Expression Omnibus; FC: FoldChange; adj. P: adjusted P; TCMSP: Traditional Chinese Medicine Systems Pharmacology Database and Analysis Platform; OB: oral bioavailability; DL: drug-likeness; DIP: Database of Interacting Proteins; BIND: Biomolecular Interaction Network Database; IntAct: IntAct Molecular Interaction Database; HPRD: Human Protein Reference Database; BioGRID: Biological General Repository for Interaction Datasets; MINT: Molecular Interaction database; DC: degree centrality; BC: betweenness centrality; BP: biological process; CC: cellular component; MF: molecular function; TNF: tumor necrosis factor; IL: interleukin; KSHV: Kaposi sarcoma-associated herpesvirus; EBV: Epstein-Barr virus; EMT: epithelial-mesenchymal transition; TGF: transforming growth factor

Cite this article as: Zhang Y, Gu L, PuYang J, Liu M, Xia Q, Jiang W, *et al*. Systems bioinformatic approach to determine the pharmacological mechanisms of *Radix Astragali* and *Radix Angelicae sinensis* in idiopathic pulmonary fibrosis. Phcog Mag 2021;17:708-18.

Correspondence:

Dr. Weilong Jiang,
Department of Respiratory Medicine, Jiangyin Hospital of Traditional Chinese Medicine, Jiangyin Hospital Affiliated to Nanjing University of Chinese Medicine, Jiangyin 214400, Jiangsu, China. E-mail: jwljytcm@163.com
Dr. Mengshu Cao,
Department of Pulmonary and Critical Care Medicine, Nanjing Drum Tower Hospital Clinical College of Traditional Chinese and Western Medicine, Nanjing University of Chinese Medicine, Nanjing 210008, Jiangsu, China.
Department of Pulmonary and Critical Care Medicine, Nanjing Drum Tower Hospital, The Affiliated Hospital of Nanjing University Medical School, Nanjing 210008, Jiangsu, China.
Department of Pulmonary and Critical Care Medicine, Nanjing Drum Tower Hospital Clinical College of Nanjing Medical University, Nanjing 210008, Jiangsu, China.
E-mail: mengshucao@126.com
DOI: 10.4103/pm.pm_9_21

Access this article online
Website: www.phcog.com
Quick Response Code:

INTRODUCTION

Idiopathic pulmonary fibrosis (IPF) is a class of chronic, progressive, fibrotic interstitial pneumonia. Pulmonary histopathology and high-resolution computed tomography existing as usual interstitial pneumonia.[1] The treatment options of IPF are imperfect, with the main drive of treatment being to interruption disease progression, recover quality of life, and prolong survival.[2] There have factually been few remedial treatment options for IPF, although efficacy has been established for pirfenidone and nintedanib in recent years.[3] Studies have recommended that traditional Chinese medicine (TCM) play a role in the treatment of IPF.[4,5]

Radix Astragali (RA) and *Radix Angelicae sinensis* (RAS) are generally employed to supplement the "qi" and activate the blood. The Danggui Buxue Decoction, which has an antiquity of numerous hundred years, is collected of RA and RAS.[6,7] RA and RAS have been revealed to decrease pulmonary fibrosis in mouse model and literature association studies have exposed that RA and RAS are the most often used herbal medicines in pulmonary fibrosis by TCM treatment.[8] Our preceding meta-analysis has shown that RA and RAS are helpful to the pulmonary function and exercise capacity of IPF patients and are operative and safe in the treatment of IPF.[9]

Network pharmacology is a frontline research field that is well-suited to studying the diverse and complex features of TCM. This tactic is now extensively applied in research on the pharmacological mechanisms of herbal medicines.[10] To date, pharmacological studies of the effect of RA and RAS on IPF have mostly engrossed on individual chemical compounds and their mechanisms of action or individual gene targets along affected pathways. Our earlier study anticipated the IPF-related target genes and the active target genes of RA and RAS from databases, following which we completed preliminary analysis to discover the mechanisms of RA and RAS acting in IPF.[8]

In the current study, we employed microarray dataset analysis combined with network pharmacology to further control the pharmacological mechanisms of RA and RAS in the treatment of IPF. First, we examined microarray datasets for differentially expressed genes (DEGs) in IPF tissues compared with normal tissues. Next, we recognized the active compounds and target genes of RA and RAS. Then, we combined the DEGs with the active target genes to paradigm a medicine-compound-gene network and protein–protein interaction (PPI) network. Then, we performed gene ontology (GO) function enrichment and Kyoto Encyclopedia of Genes and Genomes (KEGG) pathway enrichment. Finally, a gene-pathway network for IPF was positively recognized and the interactions between key compounds and their protein targets were confirmed by molecular docking.

MATERIALS AND METHODS

Searching and screening of microarray datasets

We combed microarray datasets in the National Center for Biotechnology Information (NCBI) Gene Expression Omnibus (GEO) database (https://www.ncbi.nlm.nih.gov/gds/) for gene microarrays of IPF. The recovery strategy was as follows: IPF (All Fields) AND "Homo sapiens" (porgn) AND ("gse" [Filter] AND "Expression profiling by array" [Filter]). Those datasets based on IPF clinical patients and comprising gene expression data from IPF samples and normal samples were encompassed for further analysis.

Identification of differentially expressed genes

DEGs between the IPF samples and normal samples in the microarray datasets were examined using the GEO2R online tool (https://www.ncbi.nlm.nih.gov/geo/geo2r/).[11] By comparing the IPF and normal samples, this tool generated the DEGs unswervingly. We set | log2FoldChange (FC)| >1 and adjust *P* (adj. *P*) <0.05 as the thresholds when classifying the DEGs.

Identification of active compounds and target genes of *Radix Astragali* and *Radix Angelicae sinensis*

The chemical compounds in RA and RAS were gotten from the TCM Systems Pharmacology Database and Analysis Platform (TCMSP; http://tcmspw.com/tcmsp.php).[12] The active compounds were recognized by setting oral bioavailability ≥30% and drug-likeness (DL) ≥0.18 and their conforming target genes were also gotten from TCMSP.[13] The active target genes were convert to their equivalent gene symbols from UniProt Knowledgebase (http://www.uniprot.org/).[14]

Identification of candidate target genes of *Radix Astragali* and *Radix Angelicae sinensis* acting on idiopathic pulmonary fibrosis

The active target genes of the active compounds of RA and RAS were crisscrossed with the DEGs of IPF and these intersected targets were designated as candidate target genes of RA and RAS acting on IPF.

Construction of medicine-compound-target network and selection of key compounds

We created the medicine-compound-target network using Cytoscape 3.6.0 software (Cytoscape Consortium, San Diego, CA, USA, 2017) and examined the network using the Network Analyzer tool function in Cytoscape.[15] The nodes signify the compounds and their target genes, while the edges characterize the relationship between the compounds and target genes.

Based on the linking degree between the compounds and target genes, the key compounds of RA and RAS acting on IPF were nominated.

Construction of protein–protein interaction network and selection of key interaction proteins

We employed the BisoGenet plugin of Cytoscape to construct a PPI network of the candidate target genes.[16] BisoGenet recovers the interactions among noteworthy genes or proteins from high-throughput experiments and literature data stored in six PPI databases, comprising the Database of Interacting Proteins (DIP), the Biomolecular Interaction Network Database (BIND), the IntAct Molecular Interaction Database (IntAct), the Human Protein Reference Database (HPRD), the Biological General Repository for Interaction Datasets (BioGRID) and the Molecular Interaction database (MINT). In the PPI network, the nodes characterize proteins and the edges signify interactions between them.

The core PPI network was partitioned after building a primitive PPI network. The topological properties of every node in the interaction network were examined after calculating the degree centrality (DC) and betweenness centrality (BC) with the CytoNCA plugin of Cytoscape. The definitions and computational equations of the two parameters signify the topological importance of a node in the network. More important nodes have higher quantitative values in the network. We set the DC values >61 and BC values >600 to paradigm the core PPI network.

The interaction target proteins of RA and RAS acting on IPF in the PPI network were then designated conferring to the DC values of each protein in the PPI network.

Gene ontology function enrichment and Kyoto Encyclopedia of Genes and Genomes pathway enrichment analysis

The Entrez IDs of the candidate target genes of RA and RAS acting on IPF were gotten using RGUI 3.6.1 (R Core Team, 2019) and the org. Hs. e.g. db package. Then, RGUI and the cluster Profiler package were employed to do GO function enrichment analysis, which comprise biological process (BP), cellular component (CC), and molecular function (MF) and KEGG pathway enrichment analysis.[17] By inserting the names of the candidate target genes into the ClueGO plugin of Cytoscape and editing the networks with the CluePedia plugin of Cytoscape,[18,19] the GO function enrichment and KEGG pathway enrichment were showed more spontaneously. Adjusted $P < 0.05$ was measured statistically significant.

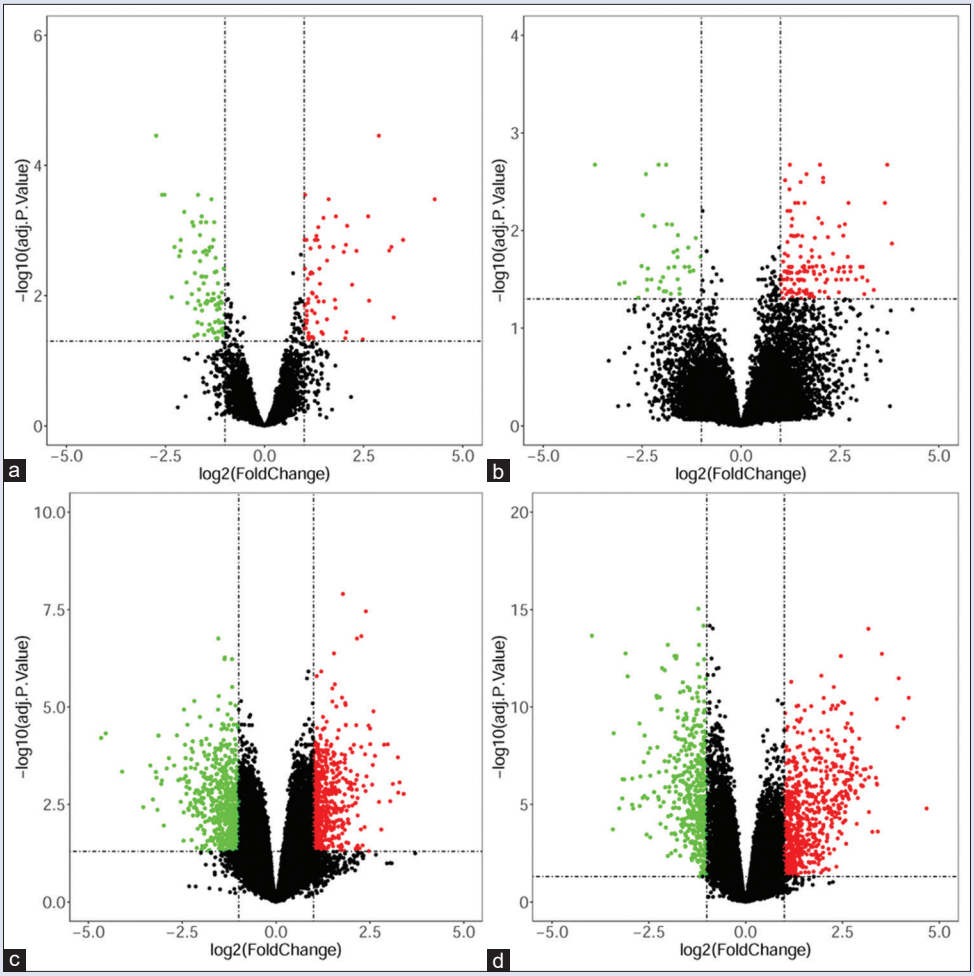

Figure 1: Differentially expressed genes between the idiopathic pulmonary fibrosis samples and normal samples. The differentially expressed genes were screened for in four microarray datasets, namely (a) GSE2052, (b) GSE21369, (c) GSE24206 and (d) GSE53845. When identifying the differentially expressed genes, |log2FC| >1 and adj. *P* <0.05 were set as the thresholds. The red and green dots represent the upregulated and downregulated genes in the idiopathic pulmonary fibrosis samples, respectively; the black dots represent mRNAs that are not differentially expressed between the IPF and normal samples

Construction of gene-pathway network

The gene-pathway network was created with Cytoscape and examined using the Network Analyzer tool. The nodes signify genes and pathways, while the edges characterize the relationships between genes and pathways.

Verification of molecular docking

The binding of the target proteins and their consistent components was confirmed by molecular docking. The structures of the compounds were attained from the PubChem Database (https://pubchem.ncbi.nlm.nih.gov/) and the target protein receptors were acquired from the RCSB PDB database (http://www.rcsb.org/). Molecular docking simulations of target protein receptors and their corresponding compounds were executed using AutoDock Tool 1.5.6 and AutoDock Vina 1.1.2 (Molecular Graphics Laboratory, The Scripps Research Institute, 2011) and further demonstration was using the PyMOL Molecular Graphics System (Version 2.4.0, Schrödinger, LLC.).[20]

Statistical analysis

Some statistical analysis was achieved automatically using the bioinformatic tools of the platforms and software stated above. When conducting differential expression analysis, |log2FC| >1 and adjusted $P < 0.05$ were measured statistically significant. In GO function and KEGG pathway enrichment analysis, adjusted $P < 0.05$ was measured statistically significant.

RESULTS

Screened microarray datasets

Four microarray datasets (GSE2052, GSE21369, GSE24206, and GSE53845) encountered the inclusion criteria and were nominated for subsequent analysis. All of these datasets enclosed gene expression data from both IPF samples and normal samples. Dataset GSE2052 is based on the GPL1739 platform (Amersham Biosciences CodeLink Uniset Human I Bioarray), GSE21369 is based on the GPL570 platform ([HG-U133_Plus_2] Affymetrix Human Genome U133 plus 2.0 Array), GSE24206 is also based on the GPL570 platform, and GSE53845 is based on the GPL6480 platform (Agilent-014850 Whole Human Genome Microarray 4 × 44K G4112F; Probe Name version). The basic evidence concerning these microarray datasets is delivered.

Identified differentially expressed genes

The four microarray datasets were designated for the screening of DEGs between IPF samples and normal samples using the GEO2R online tool. Setting adjusted $P < 0.05$ and | log2FC| >1 as the thresholds, DEGs in

Table 1: Basic information regarding the active compounds

Medicine	Active compound	Compound ID	OB (%)	DL
RA	Mairin	MOL000211	55.38	0.78
RA	Jaranol	MOL000239	50.83	0.29
RA	Hederagenin	MOL000296	36.91	0.75
RA	(3S,8S,9S,10R,13R,14S,17R)-10,13-dimethyl-17-[(2R,5S)-5-propan-2-yloctan-2-yl]-2,3,4,7,8,9,11,12,14,15,16,17-dodecahydro-1H-cyclopenta[a]phenanthren-3-ol	MOL000033	36.23	0.78
RA	isorhamnetin	MOL000354	49.6	0.31
RA	3,9-di-O-methylnissolin	MOL000371	53.74	0.48
RA	5'-hydroxyiso-muronulatol-2',5'-di-O-glucoside	MOL000374	41.72	0.69
RA	7-O-methylisomucronulatol	MOL000378	74.69	0.3
RA	9,10-dimethoxypterocarpan-3-O-β-D-glucoside	MOL000379	36.74	0.92
RA	(6aR,11aR)-9,10-dimethoxy-6a, 11a-dihydro-6H-benzofurano[3,2-c] chromen-3-ol	MOL000380	64.26	0.42
RA	Bifendate	MOL000387	31.1	0.67
RA	Formononetin	MOL000392	69.67	0.21
RA	Isoflavanone	MOL000398	109.99	0.3
RA	Calycosin	MOL000417	47.75	0.24
RA	Kaempferol	MOL000422	41.88	0.24
RA	FA	MOL000433	68.96	0.71
RA	(3R)-3-(2-hydroxy-3,4-dimethoxyphenyl) chroman-7-ol	MOL000438	67.67	0.26
RA	Isomucronulatol-7,2'-di-O-glucosiole	MOL000439	49.28	0.62
RA	1,7-Dihydroxy-3,9-dimethoxy pterocarpene	MOL000442	39.05	0.48
RA	Quercetin	MOL000098	46.43	0.28
RAS	Beta-sitosterol	MOL000358	36.91	0.75
RAS	Stigmasterol	MOL000449	43.83	0.76

RA: *Radix astragali; RAS: Radix angelicae sinensis*; OB: Oral bioavailability; DL: Drug-likeness

Table 2: Gene symbols and Entrez IDs of the candidate target genes

Gene symbol	Entrez ID
PTGS2	5743
CHRM3	1131
ADRA1A	148
ADRA1B	147
SLC6A4	6532
JUN	3725
ADRA2A	150
PLAU	5328
MAOA	4128
ADRB1	153
CCNA2	890
ND6	4541
MMP1	4312
CYP3A4	1576
SELE	6401
VCAM1	7412
CYP1B1	1545
HAS2	3037
AKR1C3	8644
MMP3	4314
CCND1	595
IL6	3569
TP63	8626
TOP1	7150
HIF1A	3091
CAV1	857
MYC	4609
CCL2	6347
MGAM	8972
SERPINE1	5054
COL1A1	1277
IFNGR1	3459
TOP2A	7153
NQO1	1728
COL3A1	1281
CXCL2	2920
CXCL10	3627
SPP1	6696
CTSD	1509
IRF1	3659

Table 3: Key compounds of *Radix astragali* and *Radix angelicae sinensis* acting on idiopathic pulmonary fibrosis

Medicine	Compound ID	Key compound	Degree
RA	MOL000098	Quercetin	30
RA	MOL000422	Kaempferol	10
RAS	MOL000449	Stigmasterol	8
RA	MOL000378	7-O-methylisomucronulatol	7
RA	MOL000392	Formononetin	6
RAS	MOL000358	Beta-sitosterol	6

RA: *Radix astragali*; RAS: *Radix angelicae sinensis*

each microarray dataset were recognized. After integration these DEGs and eliminating duplicates, 1566 DEGs endured and were definite as potential IPF-related genes. The volcano plots of these DEGs are revealed in Figure 1.

Identified active compounds and target genes of *Radix Astragali* and *Radix Angelicae sinensis*

We gained 87 active compounds in RA and 125 compounds in RAS using TCMSP. Setting OB ≥30% and DL ≥0.18, 20 active compounds for RA and two for RAS were recognized [Table 1]. The conforming target

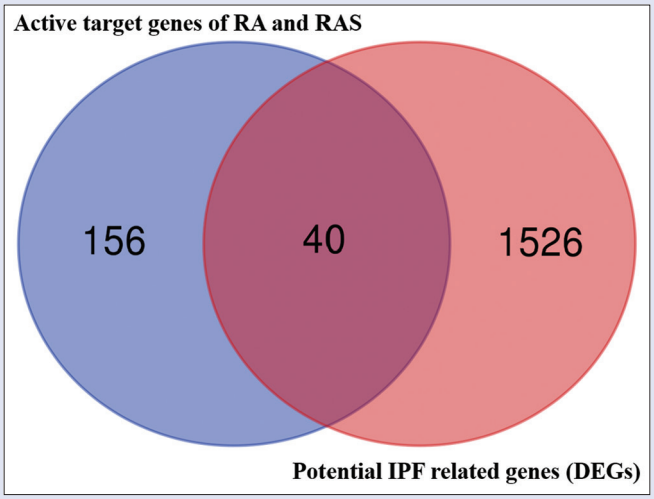

Figure 2: Candidate target genes of *Radix Astragali* and *Radix Angelicae sinensis* acting on idiopathic pulmonary fibrosis. There were 40 candidate target genes identified for *Radix Astragali* and *Radix Angelicae sinensis* in idiopathic pulmonary fibrosis treatment after 196 active target genes of *Radix Astragali* and *Radix Angelicae sinensis* were intersected with the 1566 potential idiopathic pulmonary fibrosis-related genes (differentially expressed genes between idiopathic pulmonary fibrosis and normal samples)

genes of these 22 compounds were also gained in TCMSP. The gene symbols were divided from the UniProt Knowledgebase. Four of the 22 compounds (MOL000374, MOL000398, MOL000438, and MOL000439) did not have any projected gene targets. A total of 196 target genes of RA and RAS were gotten.

Identified candidate target genes of *Radix Astragali* and *Radix Angelicae sinensis* acting on idiopathic pulmonary fibrosis

The 196 active target genes of RA and RAS were crossed with the 1566 potential IPF-related genes (DEGs), subsequent in 40 candidate target genes of RA and RAS being recognized as acting on IPF [Figure 2 and Table 2].

Constructed medicine-compound-target network and selected key compounds

The 40 candidate target genes were prophesied to respond to 15 active compounds, comprising 13 compounds in RA (MOL000239, MOL000296, MOL000354, MOL000371, MOL000378, MOL000379, MOL000380, MOL000387, MOL000392, MOL000417, MOL000422, MOL000442, and MOL000098) and two compounds in RAS (MOL000358 and MOL000449). Then, a medicine-compound-target network was created using Cytoscape software and examined with the Network Analyzer tool. There were 55 nodes (15 compound nodes, 44 target gene nodes) and 85 edges in the network [Figure 3]. The top six compounds with the highest degree in the network were MOL000098, MOL000422, MOL000449, MOL000378, MOL000392, and MOL000358 [Table 3] and these we measured to be the key compounds of RA and RAS acting on IPF.

Constructed protein–protein interaction network and selected key interaction proteins

To further study, the mechanisms of RA and RAS in the treatment of IPF, the 40 overlapping target genes were examined and a primitive PPI network was created using the BisoGenet plugin of Cytoscape. After eliminating self-loops and duplicated edges, the PPI network

was steadied and was found to comprise 2104 nodes and 50,288 edges [Figure 4a]. Next, we set the DC values to >61 to confirm proteins with significant interactions using the CytoNCA plugin, thereby assembling a PPI network that comprised 524 nodes and 21,234 edges [Figure 4b]. Finally, more suggestively interacting proteins were established after setting the BC values to >600, which produced a core PPI network of 91 nodes and 1730 edges [Figure 4c]. The interaction proteins with a high DC value in the core PPI network were recognized as the key interaction proteins in the treatment of IPF with RA and RAS. The top 15 interaction proteins in the PPI network are enumerated in Table 4.

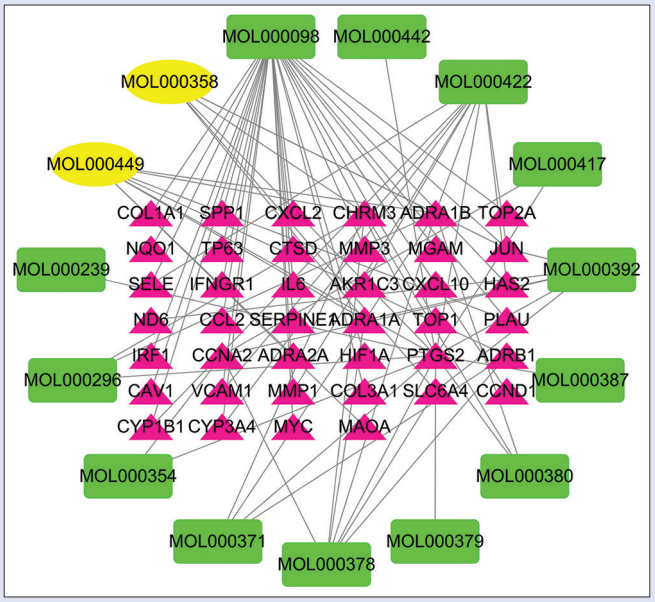

Figure 3: Construction of the medicine-compound-target network. There were 55 nodes (15 compound nodes, 40 target gene nodes) and 85 edges in the network. Rectangles represent *the Radix Astragali* compounds, ellipses represent the *Radix Angelicae sinensis* compounds, triangles represent the candidate target genes and the edges represent links between the nodes

Gene ontology function enrichment analysis

The Entrez IDs of the candidate target genes of RA and RAS acting on IPF were attained, as exposed in Table 2.

The GO BP analysis presented that the candidate target genes of RA and RAS acting on IPF were knowingly augmented for those convoluted in the regulation of body fluid levels, response to nutrients, response to reactive oxygen species and oxidative stress, extracellular matrix organization, response to nutrient levels and extracellular stimulus, extracellular structure organization, vasoconstriction, and the negative regulation of blood vessel diameter among others. The top 20 GO BP enrichments ranked based on their adjusted *P* value are revealed in Figure 5a.

GO CC analysis exposed that the candidate target genes of RA and RAS acting on IPF were suggestively enriched for genes linked with the plasma membrane raft, membrane raft, membrane microdomain, membrane region, caveola, fibrillar collagen trimer, banded collagen fibril, extracellular matrix, endoplasmic reticulum lumen, and nuclear chromatin among others. The top 20 GO CC enrichments ranked based on their adjusted *P* value are publicized in Figure 5b.

Table 4: The top 15 proteins identified in the protein–protein interaction network of *Radix astragali* and *Radix angelicae sinensis* treatment of idiopathic pulmonary fibrosis

Key interaction protein	Degree	Betweenness
NTRK1	733	7931.876
MYC	595	2676.612
CUL3	519	5684.247
FN1	490	3374.831
TP53	474	5452.51
VCAM1	451	2792.967
MCM2	439	4288.672
ITGA4	429	3401.333
ESR1	403	4980.475
APP	389	2054.432
CDK2	387	3847.213
EGFR	378	1802.213
CUL7	378	2793.545
COPS5	355	2961.508
CUL1	344	2722.892

EGFR: Estimated glomerular filtration rate

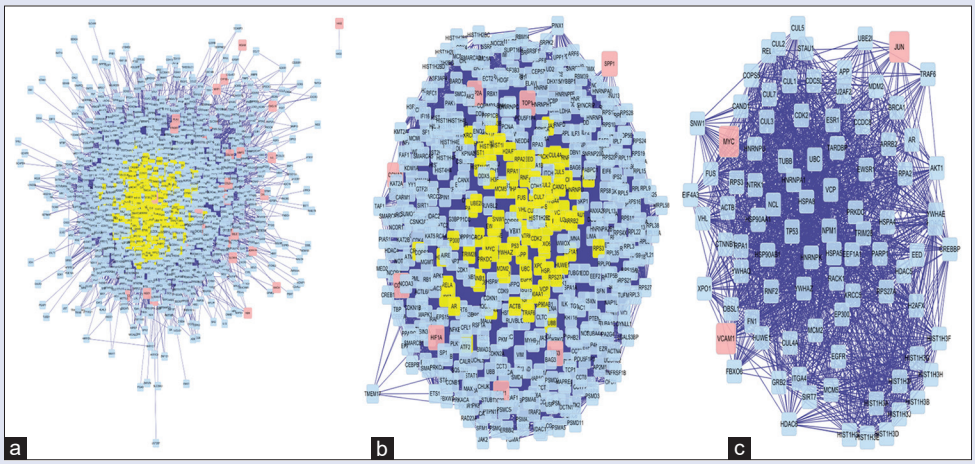

Figure 4: The protein–protein interaction network of *Radix Astragali* and *Radix Angelicae sinensis* acting on idiopathic pulmonary fibrosis. (a) Protein–protein interaction network with 2104 nodes and 50,288 edges after removing the self-loops and duplicated edges. (b) Protein–protein interaction network with 524 nodes and 21,234 edges after setting the degree centrality values to >61. (c) Protein–protein interaction network with 91 nodes and 1730 edges after setting the degree centrality values to >61 and betweenness centrality values to >600

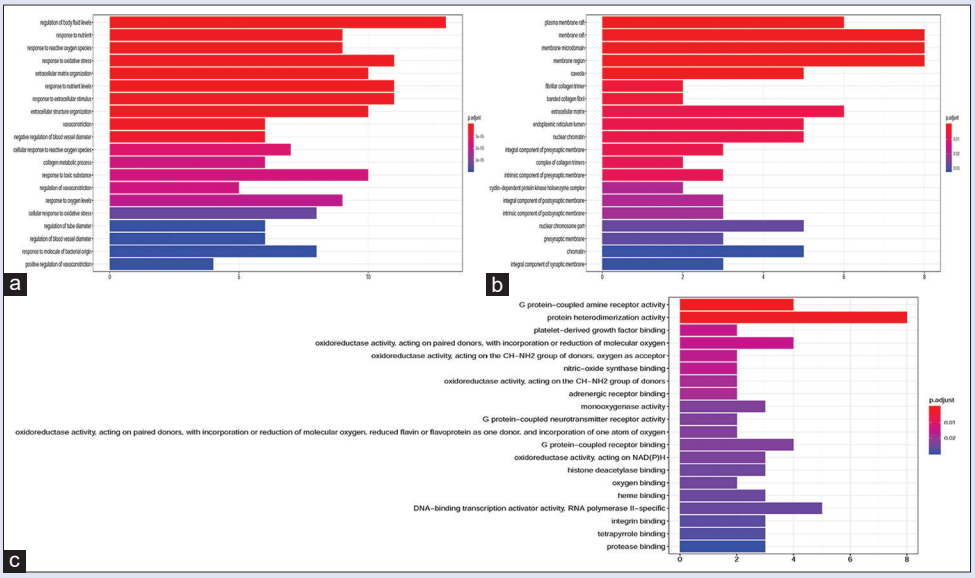

Figure 5: The top 20 gene ontology function enrichments. (a) The top 20 enriched biological process functions of the candidate target genes. (b) The top 20 enriched cellular component functions of the candidate target genes. (c) The top 20 enriched molecular functions of the candidate target genes

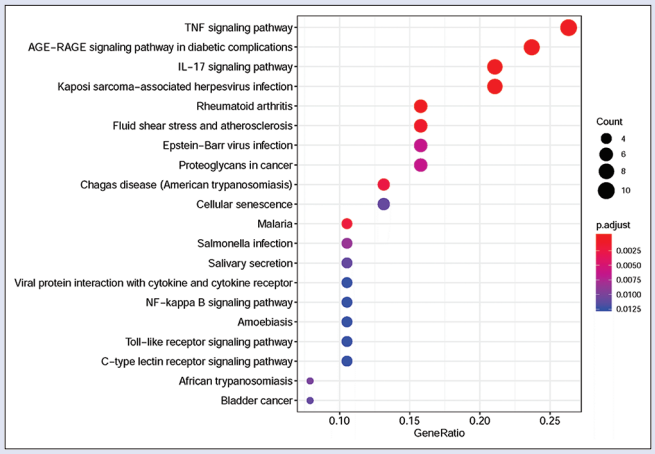

Figure 6: The top 20 Kyoto Encyclopedia of Genes and Genomes pathway enrichments

GO MF analysis disclosed that the candidate target genes of RA and RAS acting on IPF were ominously enriched for genes involved in G protein-coupled amine receptor activity, protein heterodimerization activity, platelet-derived growth factor binding, oxidoreductase activity acting on paired donors with the amalgamation or lessening of molecular oxygen, oxidoreductase activity acting on the CH-NH_2 group of donors with oxygen as the acceptor, nitric-oxide synthase binding, oxidoreductase activity acting on the CH-NH_2 group of donors, adrenergic receptor binding, monooxygenase activity, and G protein-coupled neurotransmitter receptor activity among others. The top 20 GO MF enrichments ranked based on their adjusted *P* value are presented in Figure 5c.

Using the ClueGO and CluePedia plugins of Cytoscape, the GO function enrichment from ClueGO analysis could be showed more innately, as shown in Figure S1.

Kyoto Encyclopedia of Genes and Genomes pathway enrichment analysis

The candidate target genes of RA and RAS performing on IPF were found to be expressively enriched for genes related with the tumor necrosis factor (TNF) signaling pathway, advanced glycation end (AGE) products receptor for AGE (RAGE) signaling pathway in diabetic complications, interleukin (IL)-17 signaling pathway, Kaposi sarcoma-associated herpesvirus (KSHV) infection, rheumatoid arthritis, fluid shear stress and atherosclerosis, malaria, Chagas disease (American trypanosomiasis), Epstein–Barr virus (EBV) infection, and proteoglycans in cancer among others. The top 20 KEGG pathway enrichments ranked based on their adjusted *P* value are exposed in Table 5 and Figure 6.

Using the ClueGO and CluePedia plugins of Cytoscape, the KEGG pathway enrichment from ClueGO analysis could be presented more naturally, as exposed in Figure S2.

Constructed gene-pathway network

Using the prophesied relationships between the genes and pathways publicized in Table 5, a gene-pathway network was created using Cytoscape and examined with the Network Analyzer tool. There were 47 nodes (20 gene nodes, 27 pathway nodes) and 107 edges in the network [Figure 7]. The two key pathways were hsa04668 and hsa04933, conforming to the TNF [Figure S3] and AGE-RAGE [Figure S4] signaling pathways, respectively.

Molecular docking

We attained the three-dimensional structures of the small-molecule compounds from the PubChem database and the macromolecular protein target receptors from the RCSB PDB database overdue to January 1, 2021. Then, molecular docking simulations of potential targets and their corresponding compounds were accomplished using AutoDock Tool and AutoDock Vina software. Finally, the binding of the target and its equivalent component was proved by molecular docking and established by the PyMOL Molecular Graphics System.

Table 5: Top 2 Kyoto Encyclopedia of Genes and Genomes pathway enrichments ranked based on their adjust *P*

ID	Pathway description	Gene	Adjust *P*	Count
Hsa04668	TNF signaling pathway	PTGS2	1.20E-08	10
		JUN		
		SELE		
		VCAM1		
		MMP3		
		IL6		
		CCL2		
		CXCL2		
		CXCL10		
		IRF1		
Hsa04933	AGE-RAGE signaling pathway in diabetic complications	JUN	5.69E-08	9
		SELE		
		VCAM1		
		CCND1		
		IL6		
		CCL2		
		SERPINE1		
		COL1A1		
		COL3A1		
Hsa04657	IL-17 signaling pathway	PTGS2	5.94E-07	8
		JUN		
		MMP1		
		MMP3		
		IL6		
		CCL2		
		CXCL2		
		CXCL10		
Hsa05167	Kaposi sarcoma-associated herpesvirus infection	PTGS2	8.94E-05	8
		JUN		
		CCND1		
		IL6		
		HIF1A		
		MYC		
		IFNGR1		
		CXCL2		
Hsa05323	Rheumatoid arthritis	JUN	0.000154	6
		MMP1		
		MMP3		
		IL6		
		CCL2		
		CXCL2		
Hsa05418	Fluid shear stress and atherosclerosis	JUN	0.001286	6
		SELE		
		VCAM1		
		CAV1		
		CCL2		
		NQO1		
Hsa05144	Malaria	SELE	0.002156	4
		VCAM1		
		IL6		
		CCL2		

Contd...

Table 5: Contd...

ID	Pathway description	Gene	Adjust *P*	Count
Hsa05142	Chagas disease (American trypanosomiasis)	JUN	0.002441	5
		IL6		
		CCL2		
		SERPINE1		
		IFNGR1		
Hsa05169	Epstein–Barr virus infection	JUN	0.006372	6
		CCNA2		
		CCND1		
		IL6		
		MYC		
		CXCL10		
Hsa05205	Proteoglycans in cancer	PLAU	0.006372	6
		CCND1		
		HIF1A		
		CAV1		
		MYC		
		COL1A1		
Hsa05132	Salmonella infection	JUN	0.008503	4
		IL6		
		IFNGR1		
		CXCL2		
Hsa05143	African trypanosomiasis	SELE	0.010082	3
		VCAM1		
		IL6		
Hsa04970	Salivary secretion	CHRM3	0.010921	4
		ADRA1A		
		ADRA1B		
		ADRB1		
Hsa04218	Cellular senescence	CCNA2	0.010921	5
		CCND1		
		IL6		
		MYC		
		SERPINE1		
Hsa05219	Bladder cancer	MMP1	0.010921	3
		CCND1		
		MYC		
Hsa04061	Viral protein interaction with cytokine and cytokine receptor	IL6	0.012526	4
		CCL2		
		CXCL2		
		CXCL10		
Hsa04064	NF-kappa B signaling pathway	PTGS2	0.012526	4
		PLAU		
		VCAM1		
		CXCL2		
Hsa05146	Amoebiasis	IL6	0.012526	4
		COL1A1		
		COL3A1		
		CXCL2		
Hsa04620	Toll-like receptor signaling pathway	JUN	0.012526	4
		IL6		
		CXCL10		
		SPP1		

Contd...

Table 5: Contd...

ID	Pathway description	Gene	Adjust *P*	Count
Hsa04625	C-type lectin receptor signaling pathway	PTGS2 JUN IL6 IRF1	0.012526	4

TNF: Tumor necrosis factor; AGE: Advanced glycation end; RAGE: Receptor for AGE; NF: Necrosis factor; IL: Interleukin

We nominated IL6-quercetin to validate. In the molecular docking simulations of IL6-quercetin, minimum affinity was −6.7 kcal/mol, grid center was −0.585, 0.365, and 0.253, and distance from best mode was 0.000 rmsd l. b. and 0.000 rmsd u. b [Figure 8].

DISCUSSION

IPF is an interstitial lung disease described by its chronic, progressive, and fibrotic nature.[1] Recent data have shown, TCM has played an active role in the treatment of IPF. Simple research studies have shown that TCM can expressively progress pulmonary fibrosis in animal models[21,22] and clinical studies have also exposed that TCM can recover clinical symptoms, exercise capacity, and quality of life in IPF patients.[5,23,24]

Network pharmacology is now extensively used to study herbal medicines because it is well suited to these multicomponent, multigene target, and multi-pathway target therapies.[10] In the current study, we employed microarray dataset analysis to classify IPF-regulated genes and we combined this analysis with the network pharmacology tactic to discover the pharmacological mechanism of RA and RAS in IPF treatment. We recognized 1566 DEGs and 40 candidate target genes of RA and RAS acting on IPF. The six key active compounds predicted were quercetin, kaempferol, stigmasterol, 7-O-methylisomucronulatol, formononetin, and beta-sitosterol. Following network construction and enrichment, the two main pathways were acknowledged, namely the TNF signaling pathway and AGE products receptor for AGE signaling pathway. Preliminary molecular docking to confirm interactions between key compounds and their protein targets in the pathways was carried out.

Using the network pharmacology tactic, we recognized six key compounds in RA and RAS in IPF treatment, namely quercetin, kaempferol, stigmasterol, 7-O-methylisomucronulatol, formononetin, and beta-sitosterol. Studies have revealed that quercetin can enhance pulmonary fibrosis by inhibiting SPHK1/S1P signaling,[25] augment ligand-induced apoptosis in senescent IPF fibroblasts, and decrease lung fibrosis *in vivo*.[26] Kaempferol can inhibit the epithelial–mesenchymal transition (EMT), fibrosis of the airway in endotoxin-induced epithelial cells and ovalbumin-sensitized mice.[27] The novel formononetin-7-sal ester can upgrade pulmonary fibrosis via the MEF2c signaling pathway,[28] while beta-sitosterol can inhibit transforming growth factor (TGF)-β1-induced EMT in lung alveolar epithelial cells.[29] Thus, the results of this study are in accordance with earlier studies, which designate that RA and RAS act on IPF via multiple compounds.

PPI network analysis recommended that RA and RAS act on IPF via multiple targets. The key interaction proteins recognized encompassed NTRK1, MYC, CUL3, FN1, TP53, VCAM1, MCM2, ITGA4, ESR1, APP, CDK2, EGFR, CUL7, COPS5, and CUL1 among others. Basic research studies have designated that TGF-β signaling induces HK2 accumulation in human and murine lung fibroblasts through the induction of the transcription factor, c-Myc.[30] Lung slices prepared from bleomycin-treated mice during *in vitro* incubation retain characteristics of the bleomycin model with increased expression of the fibrosis-related

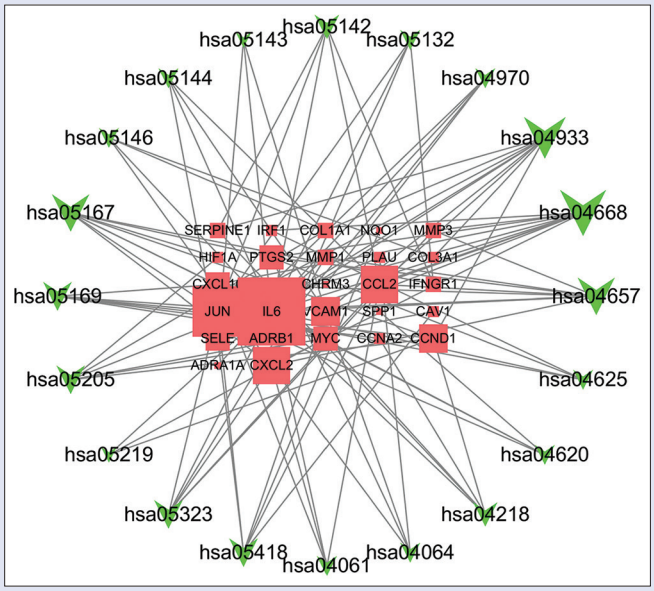

Figure 7: The gene-pathway network constructed in this study. There were 47 nodes (20 gene nodes, 27 pathway nodes) and 107 edges in the network. Rectangles represent the genes, arrows represent the pathway and edges represent the links between the nodes. The larger the nodes, the greater the connectivity

genes, ACTA2, COL1A1, FN1, MMP12, and TIMP1.[31] The TP53 gene is related with lung cancer in IPF.[32] TGF-β1 induces the upregulation of VCAM1 in IPF[33,34] and suppresses the expression of ESR family members, most particularly that of ESR1.[35] CDK2 protein expression is obviously reduced in pirfenidone-treated human prostate cancer cells,[36] while nintedanib can block EGFR paracrine upregulation in IPF fibroblasts.[37] The roles of these targets in IPF, several of which have been well studied, still merit further study, while many others endure to be discovered.

GO functional enrichment analysis proposed the enrichment of BP, CC, and MF function genes that are convoluted in aging, inflammatory response, cell proliferation, cell migration, and apoptosis, which are procedures known to underly the pathological mechanisms of IPF treatment.[38-42]

KEGG enrichment pathway analysis displayed that many pathways were thoroughly related to the pathogenesis of IPF. The relationship between many of the recognized pathways and IPF has been discovered or preliminarily established by several basic research studies. For example, fibroblast paracrine TNF-α signaling is known to raise integrin A5 expression in IPF.[43] AGE are the products of the nonenzymatic interactions between lipids and proteins during aging and RAGE is related to pulmonary fibrosis. The abnormal repairability of the IPF epithelial stroma is connected to the aging process; thus, the upsurge in AGE-RAGE signaling in IPF may be related to raised levels of epithelial stroma repair in pulmonary fibrosis.[44,45] IL-17 induces human alveolar EMT via TGF-β1-mediated SMAD2/3 and ERK1/2 activation.[46] Human EBV- and KSHV-related murine γ-herpesvirus infection can cause IPF.[47] IL-17A and prominent IL-17RA have a profibrotic effect on IPF and rheumatoid arthritis-associated lung disease.[48] Overall, these earlier results indicate that RA and RAS act on IPF via multiple pathways. The main pathways and target genes in these pathways necessitate further study.

We also accomplished molecular docking to confirm specific interactions between key compounds and their predicted protein targets in the pathways, which could recover the accuracy of the

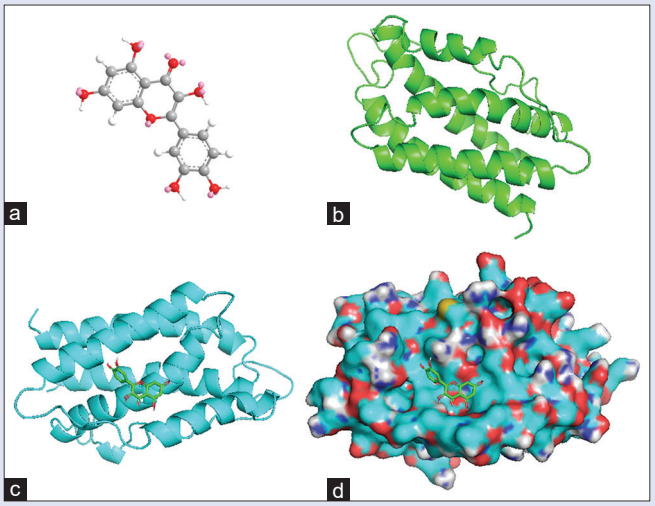

Figure 8: Interleukin 6-quercetin molecular docking. (a) Three-dimensional structures of quercetin; (b) three-dimensional structures of interleukin 6; (c) molecular docking simulation; and (d) molecular docking simulation (display protein surface)

network.[49] Preliminary molecular docking consequences show the key active compounds in RA and RAS have high binding activities with the gene target proteins. These active compounds may be some significant material basis for RA and RAS treating IPF through related signaling pathways.

Although the pharmacological mechanisms of RA and RAS in the treatment of IPF have been further dogged through the systems bioinformatic approach executed, there are still numerous limitations to this study. First, we composed microarray datasets as widely as possible and these microarray datasets are dependable; however, the number and sample sizes of these microarray datasets are lesser. Second, we recognized the active compounds and target genes of RA and RAS from TCMSP. Although this is presently the most useful database of TCM, the data collection process may still not inclusive and the screening criteria for active compounds may not be entirely precise. Finally, we only carried out preliminary molecular docking to confirm interactions between key compounds and their prophesied protein targets in the pathways, further studies *in vivo* and *in vitro* are mandatory to authenticate the target genes, key interaction proteins. and pathways acknowledged *in silico* using gene-pathway network analysis. We object to perform such studies in future.

CONCLUSION

Based on the systems bioinformatic tactic of microarray dataset analysis and network pharmacology, this study explicated the DEGs between IPF samples and normal samples and revealed the relationships among the active compounds of RA and RAS and their target genes, proteins, and pathways in IPF. Finally, the first gene-pathway network was created and preliminary molecular docking was achieved, which could prove beneficial in future studies on their mechanisms of action for the treatment of IPF. Thus, the pharmacological mechanisms of RA and RAS in IPF treatment have been further illuminated, which could demonstrate valuable in future studies for the treatment of IPF.

Acknowledgements

We would like to acknowledge the researchers who shared microarray datasets, the web database platform, and software for data analysis. We thank Natasha Beeton-Kempen, PhD, from Liwen Bianji, Edanz Editing China (www.liwenbianji.cn/ac), for editing the English text of a draft of this manuscript.

Financial support and sponsorship

This study was partially supported by the Research Grant of Jiangyin Hospital of TCM (No. 13 to Jiang and No. 14 to Zhang), the National Natural Science Foundation of China (Grant 81200049 and Grant 81670059 to Cao), and the Scientific Research Project from the Health Commission of Wuxi (Q202055 to Xia).

Conflicts of interest

There are no conflicts of interest.

REFERENCES

1. Raghu G, Remy-Jardin M, Myers JL, Richeldi L, Ryerson CJ, Lederer DJ, *et al.* Diagnosis of idiopathic pulmonary fibrosis. An official ATS/ERS/JRS/ALAT clinical practice guideline. Am J Respir Crit Care Med 2018;198:e44-68.
2. Behr J, Günther A, Bonella F, Geißler K, Koschel D, Kreuter M, *et al.* German guideline for idiopathic pulmonary fibrosis – Update on pharmacological therapies 2017. Pneumologie 2018;72:155-68.
3. Cerri S, Monari M, Guerrieri A, Donatelli P, Bassi I, Garuti M, *et al.* Real-life comparison of pirfenidone and nintedanib in patients with idiopathic pulmonary fibrosis: A 24-month assessment. Respir Med 2019;159:105803.
4. Pang LJ, Liu JP, Lv XD. Comparative effectiveness of 3 Traditional Chinese Medicine treatment methods for idiopathic pulmonary fibrosis: A systematic review and network meta-analysis protocol. Medicine (Baltimore) 2019;98:e16325.
5. Wu Q, Zhou Y, Feng FC, Zhou XM. Effectiveness and safety of Chinese medicine for idiopathic pulmonary fibrosis: A systematic review and meta-analysis. Chin J Integr Med 2019;25:778-84.
6. Shi XQ, Yue SJ, Tang YP, Chen YY, Zhou GS, Zhang J, *et al.* A network pharmacology approach to investigate the blood enriching mechanism of Danggui buxue Decoction. J Ethnopharmacol 2019;235:227-42.
7. Gong G, Qi B, Liang YT, Dong TTX, Wang HY, Tsim KWK, *et al.* Danggui Buxue Tang, an ancient Chinese herbal decoction, protects β-amyloid-induced cell death in cultured cortical neurons. BMC Complement Altern Med 2019;19:9.
8. Zhang Y, Jiang W, Xia Q, Qi J, Cao M. Pharmacological mechanism of *Astragalus* and *Angelica* in the treatment of idiopathic pulmonary fibrosis based on network pharmacology. Eur J Integr Med 2019;32:101003.
9. Zhang Y, Gu L, Xia Q, Tian L, Qi J, Cao M. Radix *Astragali* and radix *Angelicae sinensis* in the treatment of idiopathic pulmonary fibrosis: A systematic review and meta-analysis. Front Pharmacol 2020;11:415.
10. Zhang R, Zhu X, Bai H, Ning K. Network pharmacology databases for traditional Chinese medicine: Review and assessment. Front Pharmacol 2019;10:123.
11. Davis S, Meltzer PS. GEOquery: A bridge between the Gene Expression Omnibus (GEO) and BioConductor. Bioinformatics 2007;23:1846-7.
12. Ru J, Li P, Wang J, Zhou W, Li B, Huang C, *et al.* TCMSP: A database of systems pharmacology for drug discovery from herbal medicines. J Cheminform 2014;6:13.
13. Xia Q, Liu M, Li H, Tian L, Qi J, Zhang Y. Network pharmacology strategy to investigate the pharmacological mechanism of HuangQiXiXin decoction on cough variant asthma and evidence-based medicine approach validation. Evid Based Complement Alternat Med 2020;2020:1-5.
14. UniProt Consortium T. UniProt: The universal protein knowledgebase. Nucleic Acids Res 2018;46:2699.
15. Shannon P, Markiel A, Ozier O, Baliga NS, Wang JT, Ramage D, *et al.* Cytoscape: A software environment for integrated models of biomolecular interaction networks. Genome Res 2003;13:2498-504.
16. Martin A, Ochagavia ME, Rabasa LC, Miranda J, Fernandez-de-Cossio J, Bringas R. BisoGenet: A new tool for gene network building, visualization and analysis. BMC Bioinformatics 2010;11:91.
17. Yu G, Wang LG, Han Y, He QY. clusterProfiler: An R package for comparing biological themes among gene clusters. OMICS 2012;16:284-7.
18. Bindea G, Galon J, Mlecnik B. CluePedia Cytoscape plugin: Pathway insights using integrated

experimental and in silico data. Bioinformatics 2013;29:661-3.

19. Bindea G, Mlecnik B, Hackl H, Charoentong P, Tosolini M, Kirilovsky A, *et al.* ClueGO: A Cytoscape plug-in to decipher functionally grouped gene ontology and pathway annotation networks. Bioinformatics 2009;25:1091-3.
20. Trott O, Olson AJ. AutoDock Vina: Improving the speed and accuracy of docking with a new scoring function, efficient optimization, and multithreading. J Comput Chem 2010;31:455-61.
21. Yu X, Zhang Y, Yang X, Zhang X, Wang X, Liu X, *et al.* The influence of buqihuoxuetongluo formula on histopathology and pulmonary function test in bleomycin-induced idiopathic pulmonary fibrosis in rats. Evid Based Complement Alternat Med 2018;2018:8903021.
22. Chen H, Chen Q, Jiang CM, Shi GY, Sui BW, Zhang W, *et al.* Triptolide suppresses paraquat induced idiopathic pulmonary fibrosis by inhibiting TGFB1-dependent epithelial mesenchymal transition. Toxicol Lett 2018;284:1-9.
23. Chen MJ, Yang GL, Ding YX, Tong ZQ. Efficacy of TCM therapy of tonifying lung-kidney's Qi-deficiency in a case of idiopathic pulmonary fibrosis: A case report. Medicine (Baltimore) 2019;98:e15140.
24. Yu Y, Sun Z, Shi L, Zhang Y, Zhou Z, Zhang S, *et al.* Effects of feiwei granules in the treatment of idiopathic pulmonary fibrosis: A randomized and placebo-controlled trial. J Tradit Chin Med 2016;36:427-33.
25. Zhang X, Cai Y, Zhang W, Chen X. Quercetin ameliorates pulmonary fibrosis by inhibiting SphK1/S1P signaling. Biochem Cell Biol 2018;96:742-51.
26. Hohmann MS, Habiel DM, Coelho AL, Verri WA Jr., Hogaboam CM. Quercetin enhances ligand-induced apoptosis in senescent idiopathic pulmonary fibrosis fibroblasts and reduces lung fibrosis *in vivo*. Am J Respir Cell Mol Biol 2019;60:28-40.
27. Gong JH, Cho IH, Shin D, Han SY, Park SH, Kang YH. Inhibition of airway epithelial-to-mesenchymal transition and fibrosis by kaempferol in endotoxin-induced epithelial cells and ovalbumin-sensitized mice. Lab Invest 2014;94:297-308.
28. Zhao X, Qu G, Song C, Li R, Liu W, Lv C, *et al.* Novel formononetin-7-sal ester ameliorates pulmonary fibrosis via MEF2c signaling pathway. Toxicol Appl Pharmacol 2018;356:15-24.
29. Park YJ, Bang IJ, Jeong MH, Kim HR, Lee DE, Kwak JH, *et al.* Effects of β-sitosterol from corn silk on TGF-β1-induced epithelial-mesenchymal transition in lung alveolar epithelial cells. J Agric Food Chem 2019;67:9789-95.
30. Yin X, Choudhury M, Kang JH, Schaefbauer KJ, Jung MY, Andrianifahanana M, *et al.* Hexokinase 2 couples glycolysis with the profibrotic actions of TGF-β. Sci Signal 2019;12:eaax4067.
31. Cedilak M, Banjanac M, Belamarić D, Paravić Radičević A, Faraho I, Ilić K, *et al.* Precision-cut lung slices from bleomycin treated animals as a model for testing potential therapies for idiopathic pulmonary fibrosis. Pulm Pharmacol Ther 2019;55:75-83.
32. Demopoulos K, Arvanitis DA, Vassilakis DA, Siafakas NM, Spandidos DA. MYCL1, FHIT, SPARC, p16(INK4) and TP53 genes associated to lung cancer in idiopathic pulmonary fibrosis. J Cell Mol Med 2002;6:215-22.
33. Wang X, Ouyang Z, You Q, He S, Meng Q, Hu C, *et al.* Obaculactone protects against bleomycin-induced pulmonary fibrosis in mice. Toxicol Appl Pharmacol 2016;303:21-9.
34. Agassandian M, Tedrow JR, Sembrat J, Kass DJ, Zhang Y, Goncharova EA, *et al.* VCAM-1 is a TGF-β1 inducible gene upregulated in idiopathic pulmonary fibrosis. Cell Signal 2015;27:2467-73.
35. Smith LC, Moreno S, Robertson L, Robinson S, Gant K, Bryant AJ, *et al.* Transforming growth factor beta1 targets estrogen receptor signaling in bronchial epithelial cells. Respir Res 2018;19:160.
36. Ishii K, Sasaki T, Iguchi K, Kato M, Kanda H, Hirokawa Y, *et al.* Pirfenidone, an anti-fibrotic drug, suppresses the growth of human prostate cancer cells by inducing G_1 cell cycle arrest. J Clin Med 2019;8:44.
37. Epstein Shochet G, Brook E, Eyal O, Edelstein E, Shitrit D. Epidermal growth factor receptor paracrine upregulation in idiopathic pulmonary fibrosis fibroblasts is blocked by nintedanib. Am J Physiol Lung Cell Mol Physiol 2019;316:L1025-34.
38. Ma WH, Li M, Ma HF, Li W, Liu L, Yin Y, *et al.* Protective effects of GHK-Cu in bleomycin-induced pulmonary fibrosis via anti-oxidative stress and anti-inflammation pathways. Life Sci 2020;241:117139.
39. Selman M, Pardo A. The leading role of epithelial cells in the pathogenesis of idiopathic pulmonary fibrosis. Cell Signal 2020;66:109482.
40. Li J, Feng M, Sun R, Li Z, Hu L, Peng G, *et al.* Andrographolide ameliorates bleomycin-induced pulmonary fibrosis by suppressing cell proliferation and myofibroblast differentiation of fibroblasts via the TGF-β1-mediated Smad-dependent and -independent pathways. Toxicol Lett 2020;321:103-13.
41. Tisler M, Alkmin S, Chang HY, Leet J, Bernau K, Sandbo N, *et al.* Analysis of fibroblast migration dynamics in idiopathic pulmonary fibrosis using image-based scaffolds of the lung extracellular matrix. Am J Physiol Lung Cell Mol Physiol 2020;318:L276-86.
42. Zhao H, Wang Y, Qiu T, Liu W, Yao P. Autophagy, an important therapeutic target for pulmonary fibrosis diseases. Clin Chim Acta 2020;502:139-47.
43. Epstein Shochet G, Brook E, Israeli-Shani L, Edelstein E, Shitrit D. Fibroblast paracrine TNF-α signaling elevates integrin A5 expression in idiopathic pulmonary fibrosis (IPF). Respir Res 2017;18:122.
44. Kyung SY, Byun KH, Yoon JY, Kim YJ, Lee SP, Park JW, *et al.* Advanced glycation end-products and receptor for advanced glycation end-products expression in patients with idiopathic pulmonary fibrosis and NSIP. Int J Clin Exp Pathol 2014;7:221-8.
45. Machahua C, Montes-Worboys A, Llatjos R, Escobar I, Dorca J, Molina-Molina M, *et al.* Increased AGE-RAGE ratio in idiopathic pulmonary fibrosis. Respir Res 2016;17:144.
46. Wang T, Liu Y, Zou JF, Cheng ZS. Interleukin-17 induces human alveolar epithelial to mesenchymal cell transition via the TGF-β1 mediated Smad2/3 and ERK1/2 activation. PLoS One 2017;12:e0183972.
47. Dong S, Forrest JC, Liang X. Murine Gammaherpesvirus 68: A Small Animal Model for Gammaherpesvirus-Associated Diseases. Adv Exp Med Biol 2017;1018:225-36.
48. Zhang J, Wang D, Wang L, Wang S, Roden AC, Zhao H, *et al.* Profibrotic effect of IL-17A and elevated IL-17RA in idiopathic pulmonary fibrosis and rheumatoid arthritis-associated lung disease support a direct role for IL-17A/IL-17RA in human fibrotic interstitial lung disease. Am J Physiol Lung Cell Mol Physiol 2019;316:L487-97.
49. Yi P, Zhang Z, Huang S, Huang J, Peng W, Yang J. Integrated meta-analysis, network pharmacology, and molecular docking to investigate the efficacy and potential pharmacological mechanism of Kai-Xin-San on Alzheimer's disease. Pharm Biol 2020;58:932-43.